The Role of the Individual Lhcas in Photosystem I Excitation Energy Trapping

Emilie Wientjes,[†] Ivo H. M. van Stokkum,[‡] Herbert van Amerongen,[§¶] and Roberta Croce[†‡*]

[†]Department of Biophysical Chemistry, Groningen Biomolecular Sciences and Biotechnology Institute, University of Groningen, Groningen, The Netherlands; [‡]Department of Physics and Astronomy, Faculty of Sciences, VU University, Amsterdam, The Netherlands; [§]Laboratory of Biophysics, Wageningen University, Wageningen, The Netherlands; and [¶]MicroSpectroscopy Centre, Wageningen, The Netherlands

ABSTRACT In this work, we have investigated the role of the individual antenna complexes and of the low-energy forms in excitation energy transfer and trapping in Photosystem I of higher plants. To this aim, a series of Photosystem I (sub)complexes with different antenna size/composition/absorption have been studied by picosecond fluorescence spectroscopy. The data show that Lhca3 and Lhca4, which harbor the most red forms, have similar emission spectra (λ_{max} = 715–720 nm) and transfer excitation energy to the core with a relative slow rate of ~25/ns. Differently, the energy transfer from Lhca1 and Lhca2, the "blue" antenna complexes, occurs about four times faster. In contrast to what is often assumed, it is shown that energy transfer from the Lhca1/4 and the Lhca2/3 dimer to the core occurs on a faster timescale than energy equilibration within these dimers. Furthermore, it is shown that all four monomers contribute almost equally to the transfer to the core and that the red forms slow down the overall trapping rate by about two times. Combining all the data allows the construction of a comprehensive picture of the excitation-energy transfer routes and rates in Photosystem I.

INTRODUCTION

Photosystem I (PSI) is a plastocyanin: ferredoxin oxidoreductase that plays a major role in the photosynthetic light reactions in cyanobacteria, algae, and higher plants. Although cyanobacteria and plants diverged in evolution one billion years ago, they have a highly conserved PSI core complex (1,2). This pigment-protein complex coordinates ~100 chlorophylls *a* (Chls *a*), β-carotene molecules, the reaction center (RC), and all the electron transport cofactors (2). Light is harvested by the pigments and the excitation energy is transferred to the RC where it is used for charge separation. In algae and higher plants additional light-harvesting complexes (Lhcs) are present to increase the absorption cross section of PSI. In higher plants these Lhcs are composed of two heterodimers: Lhca1/4 and Lhca2/3, which are organized as a crescent shape around the core (1,3–5). A fifth complex, Lhca5 is present in substoichiometric amounts (6,7). Gap pigments are located in between the core and the Lhcas and presumably facilitate excitation-energy transfer (EET) between the different parts of the system (1). The supercomplex composed of PSI core and all four Lhcs (PSI-LHCI) coordinates ~170 Chls *a* and *b* and carotenoids: β-carotene, violaxanthin, and lutein (8–10).

A special feature of almost all PSI complexes is the presence of the red forms: Chls that absorb at longer wavelengths than the RC (11,12). Thus, EET from these Chls to the RC is energetically uphill and needs to be thermally activated (13). Even though uphill EET slows down the trapping rate, the quantum efficiency of PSI is still extremely high (11,14). In higher plant PSI some red forms are located in the core, and are responsible for the 720 nm low-temperature (LT) fluorescence emission, but most red forms are coordinated by LHCI (15,16). In vitro reconstitution studies have shown that Lhca3 and Lhca4 coordinate Chls that absorb at 705–710 nm and emit at 725–735 nm (10,17,18). Furthermore, Lhca2 shows a red-shifted LT emission maximum (compared to 680 nm observed for PSII antenna) at 701 nm (17), which arises from an absorption band at 690 nm (19). Lhca1 has its emission maximum at 690 nm and a shoulder at 701 nm (20). It has been shown that the red-shifted absorption of Lhca complexes arises from the lowest exciton state of two strongly coupled Chls *a* (603 and 609 (nomenclature as in (21)) (19,20,22–24)) mixed with a charge-transfer state (25).

The presence of red forms in the native Lhca1/4 dimer has been known for a long time (10), in contrast to the presence of red forms in Lhca2/3, which was more controversial and could only recently be confirmed (5). It was shown that the red form content in Lhca1/4 and Lhca2/3 is practically identical, and that they show 77 K emission maxima at 731.5 and 728.5 nm, respectively (5,26). Due to their low excited-state energy, red forms have an important effect on EET and trapping in PSI. Indeed, at room temperature (RT) they give rise to 80% of the fluorescence emission of higher plant PSI (27).

The function of the red forms is not fully understood, it has been proposed that they play a role in photoprotection, concentration of the excitation energy and/or strongly contribute to the PSI absorption under specific light conditions (28–31).

The EET and trapping processes in PSI have been studied extensively by time-resolved techniques: transient absorption, fluorescence upconversion, synchroscan streak camera, and time-correlated single photon counting (TCSPC).

Submitted May 3, 2011, and accepted for publication June 24, 2011.

*Correspondence: r.croce@vu.nl

Editor: Leonid S. Brown.

0006-3495/11/08/0745/10 $2.00

doi: 10.1016/j.bpj.2011.06.045

Gobets et al. (32) studied a range of PSI complexes from cyanobacteria with different red form content and found that the excitation energy trapping of all complexes could be described with a lifetime of 18 ps and an additional slower component. The lifetime and amplitude of the slower component correlate with the amount and energy of the red forms. The main fluorescence decay time of the higher plant PSI cores is ~18 ps (33,34), while it is still unknown whether a second slower lifetime is needed to describe the red form decay kinetics.

Time-resolved fluorescence studies on PSI-LHCI from higher plants have shown that, compared to the purified core, additionally red-shifted decay-associated spectra (DAS) are needed to describe the data (13,33–37). The exact lifetimes and DAS differ from study to study, probably reflecting a high sensitivity of PSI to handling and measuring conditions, but most studies show a similar trend: a fast ~5–10 ps bulk/red energy equilibration component, a ~20- ps trapping component with a PSI core-like spectrum, and at least one red-shifted DAS with lifetimes $\geq$ 55 ps. In some studies a smaller number of components is used to describe the data (33,35), but most likely these DAS represent an average of components that are resolved in the other reports.

In the past decade it has become clear that the slow phase in the PSI-LHCI fluorescence decay is related to the low energy Chls in LHCI (13,33,35,36,38,39), in particular of Lhca3 and Lhca4 (34). So far, however, there is no agreement about the spectra and decay kinetics of the individual Lhcas when associated with the core (34,36,37,39,40). This is mainly because PSI is a very large and complex system, making it difficult to extract the details from the decay kinetics. To tackle this problem and to improve the understanding of EET in PSI-LHCI we have chosen a systematic approach. First, to reduce the complexity, we purified the major PSI building blocks: Lhca1/4, Lhca2/3, and core and studied their time-resolved fluorescence dynamics. Next, we gradually increased the complexity, by "rebuilding" the system, making use of PSI from a mutant plant that consists of a PSI core, only coordinating the Lhca1/4 dimer (41–43), and finally studying the wild-type (WT) complex. In addition, to specifically investigate the role of the red forms we studied a complex in which Lhca4 (with red forms) is substituted by Lhca5 (without red forms) (43).

MATERIALS AND METHODS

Isolation of PSI complexes

All complexes were obtained from *Arabidopsis thaliana* plants. Lhca1/4 and Lhca2/3 were isolated as described in (5) and the PSI core was obtained as in (15). PSI complexes were obtained from WT, Lhca2 antisense, and Lhca4 knockout plants (44,45) as described previously (43). All complexes were separated by sucrose density ultracentrifugation, on a 0.1–1 M sucrose gradient with 0.03% *n*-dodecyl-α-D-maltoside and 10 mM tricine, pH 7.8. PSI complexes were further purified by one (PSI-WT, PSI Lhca2 antisense) or two (PSI Lhca4 knockout) subsequent sucrose gradients. After harvesting, the complexes were snap frozen in N_2(l) and stored at 193 K.

All spectroscopic measurements were performed in 0.5 M sucrose, 0.03% *n*-dodecyl-α-D-maltoside, and 10 mM tricine pH 7.8.

Steady-state spectroscopy

Absorption spectra were recorded on a Cary 4000 UV-Vis spectrophotometer (Varian, Palo Alto, CA). Fluorescence spectra were recorded on a Fluorolog 3.22 spectrofluorimeter (HORIBA Jobin Yvon, Longjumeau, France). Intactness of the sample was checked by recording the steady-state emission spectra before and after time-resolved fluorescence measurements. No significant changes were observed.

TCSPC

TCSPC was performed at 283 K with a homebuilt setup, as described previously (46). Excitation was performed with a light pulse at 440 or 475 nm and a repetition rate of 3.8 MHz. Pulse energies of (sub)-picojoules were used with pulse duration of 0.2 ps and a spot diameter of 2 mm. The instrument response function (~80 ps at full width half maximum) was obtained with pinacyanol iodide in methanol, with a 6-ps fluorescence lifetime (37). A channel time spacing of 2 ps was used, resulting in an 8-ns time window. Further experimental settings were as in (26). The steady-state fluorescence emission spectra were used to calculate the DAS.

Calculation of LHCI to core migration time

Based on the fractions of PSI core and LHCI excitation at two different excitation wavelengths (see Section SI. 2 in the Supporting Material) and the respective average fluorescence lifetimes, the fluorescence lifetime upon selective excitation of only LHCI ($\overline{\tau}_L$) or only PSI core ($\overline{\tau}_C$) can be calculated (37). The average fluorescence lifetime is the sum of the trapping time, which is independent of the location of the initial excitation, and the migration time. Thus, the difference between $\overline{\tau}_L$ and $\overline{\tau}_C$, given by Eq. 1, can be attributed to the extra migration time from LHCI to the core (37).

$$\overline{\tau}_{L-C} = \frac{<\tau>_{475} - <\tau>_{440}}{ExLHCI_{475} - ExLHCI_{440}}, \quad (1)$$

with $\overline{\tau}_{L-C}$ being the difference in average lifetime after excitation of LHCI or core. $<\tau>_{\#\#\#}$ is the average fluorescence lifetime after excitation at ### nm. And $ExLHCI_{\#\#\#}$ is the fraction of excitation that is created on LHCI upon ### nm excitation.

Synchroscan streak camera measurement and modeling

Streak-camera fluorescence measurements were performed (at 295 K) with a set of lasers and a synchroscan streak-camera detection system, as described in (47). Excitation was at 475 nm and a time window of 160 ps was used. Further experimental settings and data analysis were as in (26). Target analysis yielded the species associated spectra of the transfer rates between the red Lhca, blue Lhca, core bulk, and core red compartment; for details on target analysis see (48). To reduce the number of free fit parameters the spectrum of blue antenna is taken to be the same as the bulk core spectrum, the red antenna emission is 0 for $\lambda < 680$ nm, the red core emission is 0 for $\lambda < 695$ nm. For PSI-WT the initial excitation fraction of the core was fixed at 35% as obtained from the absorption spectra (Table 1). LHCI excitation was 65%, the fractions of red versus blue antenna excitation were estimated at 0.22 and 0.78, indicating that the red Lhca compartment represents the red forms and the Chls nearby.

TABLE 1 TCSPC fluorescence decay parameters of PSI complexes

PSI core			PSI-Lhca1/4			PSI-WT			PSI-Lhca5		
τ	A_{440}	A_{475}	τ	A_{440}	A_{475}	τ	A_{440}	A_{475}	τ	A_{440}	A_{475}
18 ps	88%	84%	23 ps	69%	59%	20 ps	54%	45%	26 ps	67%	65%
44 ps	11%	16%	89 ps	25%	35%	83 ps	43%	51%	78 ps	29%	32%
0.28 ns	0.3%	0.4%	0.29 ns	2.3%	3.0%	0.23 ns	2.7%	2.9%	0.47 ns	2.2%	1.3%
2.4 ns	0.1%	0.2%	2.3 ns	1.6%	2.4%	1.7 ns	0.2%	0.2%	3.1 ns	1.7%	1.9%
5.2 ns	0.4%	0.1%	5.5 ns	1.8%	0.8%	5.3 ns	0.3%	0.1%	8.9 ns	0.4%	0.3%
$<\tau>$* (ps)	21.3	22.9		46.6	55.5		52.9	58.4		41.4	42.7
$\tau_{475\text{-}440}$ (ps)		1.6			8.9			5.5			1.3
Ex core	100%	100%		76%	47%		62%	35%		61%	38%
$\overline{\tau}_C$ (ps)					39.0			45.5			39.2
$\overline{\tau}_L$ (ps)					70.3			65.1			44.9
$\overline{\tau}_{L-C}$ (ps)					31			20			6

$A_{440,475}$ is the relative contribution to fluorescence decay based on area under DAS after excitation at 440 or 475 nm. The underlined lifetimes are used to calculate the average lifetimes:

$$<\tau> = \sum_{i=1}^{3} A_i^* \tau_i.$$

Fraction of core excitation is indicated, see Section SI. 2 in the Supporting Material for details. $\overline{\tau}_C$ is the calculated lifetime for hypothetical selective excitation of the core, and $\overline{\tau}_L$ for selective excitation of LHCI, $\overline{\tau}_{L-C}$ is the migration time from LHCI to the core.

The dissipative rate of purified Lhca1/4 was 0.47/ns: this loss rate was used for all compartments.

RESULTS

Red forms of PSI complexes studied with LT fluorescence

Fig. 1 shows the LT emission of Lhca1/4, PSI core, PSI-Lhca1/4, and PSI-Lhca1/4-Lhca2/3 (further called PSI-WT) (the absorption spectra are reported in Section SI. 1 of the Supporting Material). The emission maximum of PSI-Lhca1/4 is a few nm blue-shifted as compared to PSI-WT indicating that in the case of PSI-Lhca1/4 relatively more emission is coming from the core (41). Because contamination of the PSI-Lhca1/4 preparation with PSI-core can be excluded (43), the data indicates that the EET between the core and Lhca1/4 in PSI-Lhca1/4 is not as good as in the WT complex.

The low fluorescence intensity in the 680-nm region observed for all complexes, shows that most pigments transfer their excitation energy to the red forms, meaning that the samples are virtually free of PSII contaminations and/or uncoupled Chls.

Fluorescence decay dynamics: streak camera measurements

The fluorescence dynamics of the complexes (Fig. 2 *A*) were studied at room temperature with the synchroscan streak camera, after excitation at 475 nm. It is immediately clear from the streak images that the fluorescence of the Lhca1/4 dimer shows hardly any decay on the 140-ps timescale, only energy equilibration between the bulk pigments and the red forms can be observed (Fig. 2 *B*). The PSI core on the other hand decays extremely fast (Fig. 2 *B*). When the Lhca1/4 dimer is associated with the core (PSI-Lhca1/4) the fluorescence decay is still fast, although slightly slower than for the PSI core and it shows stronger emission at the longer wavelengths (~720 nm) (Fig. 2 *B*). Furthermore, if the Lhca2/3 dimer is associated with the core (PSI-WT) an additional increase in the longer wavelengths emission is observed (Fig. 2 *B*). The fast decay of PSI-Lhca1/4 and PSI-WT as compared to Lhca1/4 indicates that in these complexes the excitation energy is efficiently transferred from Lhcas to the core and subsequently trapped by the RC.

To investigate the effect of the LHCI antenna on the fluorescence decay in a quantitative way the DAS were estimated (Fig. 2 *C*). The DAS associated with the shortest lifetimes (3–13 ps) have spectra with a positive contribution around ~680 nm and a negative one around ~720 nm for all complexes. This is typical for PSI complexes and represents energy equilibration between the bulk pigments and the

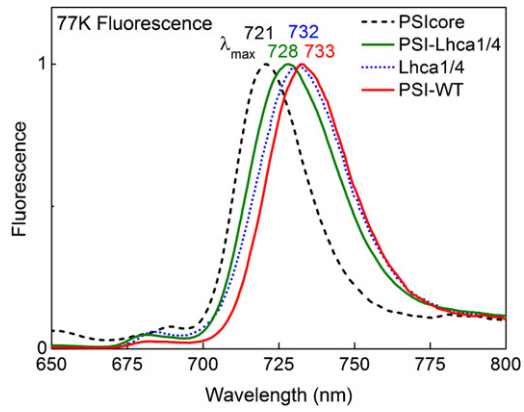

FIGURE 1 77 K fluorescence emission of PSI (sub)complexes upon 475 nm excitation.

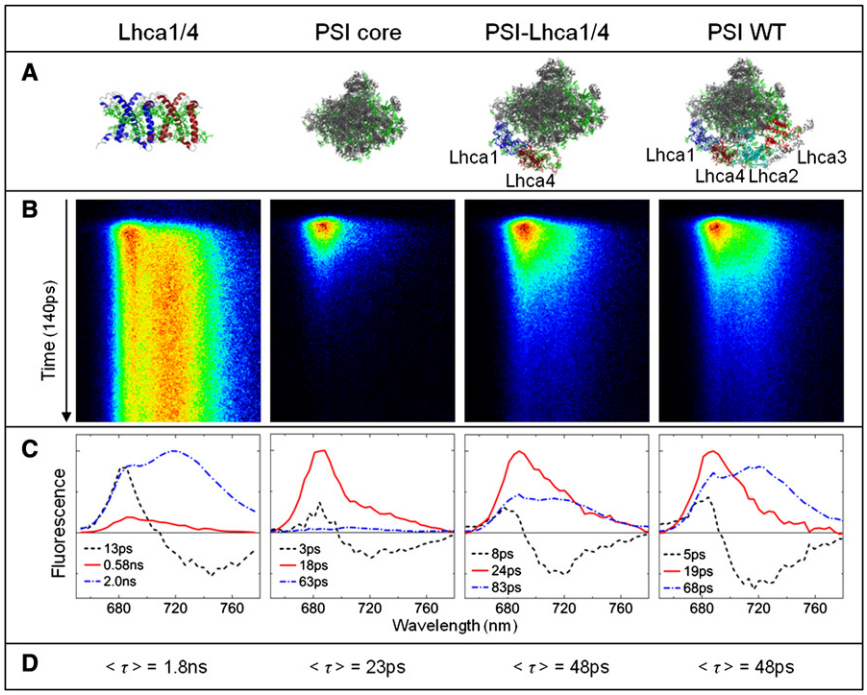

FIGURE 2 Streak-camera time-resolved fluorescence measurements. (*A*) Cartoons of the investigated complexes were prepared with PyMOL (DeLano, W. L. The PyMOL Molecular Graphics System (2002) on http://www.pymol.org) from the structural data of PSI-LHCI (57) (and LHCII (21) for Lhca1/4) (Protein Data Bank codes: 2O01 and 1RWT). (*B*) Streak images showing 140 ps along the *y* axis and 650–780 nm along the *x* axis. Color represents fluorescence intensity with black no fluorescence, red highest intensity. Excitation was at 475 nm. (*C*) DAS estimated from the streak data, shown in *B*. (*D*) Average lifetime calculated according to $\tau_{av} = \Sigma A_i * \tau_i$, with *A* the relative area under the DAS and τ the corresponding lifetime, the transfer component was not taken into account.

low-energy forms. In Lhca1/4 the main fluorescence decay occurs with a 2-ns lifetime and the DAS shows a maximum around 720 nm due to emission from the low-energy Chls. A fraction of Lhca1/4 decays faster (0.58 ns), which presumably arises from complexes in a quenched conformation (26). The PSI core decays mainly with an 18-ps lifetime, as observed previously (33,34). In addition, a small contribution of a 63-ps component with red emission is observed due to the presence of red forms in the core (see LT emission (Fig. 1) and (11,15)). For PSI-Lhca1/4 a 24-ps component with a similar spectrum as the 18-ps core DAS is present together with an 83-ps DAS resembling the 2 ns DAS of Lhca1/4. In PSI-WT similar DAS as in PSI-Lhca1/4 were observed, but the amplitude of the Lhca1/4-like DAS increased, although its lifetime was somewhat shorter (68 ps). It can thus be concluded that both Lhca2/3 and Lhca1/4 contribute to the amplitude of the red-shifted DAS. The average lifetime of the complexes (Fig. 2 *D*) increases from 20 ps for PSI core, to 48 ps for PSI-WT. PSI-Lhca1/4 also has an average lifetime of 48 ps, which is surprising considering the smaller number of Chls and red forms in PSI-Lhca1/4.

TCSPC after preferential core and antenna excitation

The fluorescence decay of the complexes was also investigated by TCSPC (at 283 K). This technique is more sensitive than the streak camera allowing for a more accurate estimation of the fluorescence lifetimes. A disadvantage is the broader instrument response function that results in a lower time resolution, hampering the resolution of the blue to red EET component (3–8 ps in the PSI complexes, Fig. 2).

TCSPC measurements were performed after excitation at 440 nm (exciting mainly Chl *a* and Cars) and 475 nm (exciting Chl *b* and Cars). Because Chl *b* is only present in LHCI, 475 nm excitation is more selective for the antenna, while 440 nm is preferentially exciting the core complex, see Section SI. 2 in the Supporting Material.

Fig. 3 shows the DAS estimated from the TCSPC measurements of: PSI-core, PSI-Lhca1/4, and PSI-WT complexes. Due to the rather broad global fit minimum (33) various combinations of amplitude and lifetimes can describe the data; to be able to compare the relative amplitudes, the two sets of measurements (440- and 475-nm excitation) were fitted simultaneously. For all complexes five lifetimes were needed to describe the data; the fastest three (ps to sub-ns) were attributed to PSI, whereas two long lifetime components (ns) with very small amplitudes were ascribed to PSII contaminations/free Chls.

The decay of the core is mainly described with an 18-ps lifetime (Fig. 3 *A*, Table 1). In addition two red DAS, with lifetimes 44 ps (amplitude 11% for 440-nm excitation) and 0.28 ns (amplitude 0.3%) are needed to describe the data (Table 1). The longer components are ascribed to red forms in the core (Fig. 1), because the sample is not notably contaminated with PSI-LHCI, as can be judged from LT emission (Fig. 1) and protein analysis (see Fig. 4 in (43)). Interestingly, upon excitation at 475 nm the contribution of the red component increased as compared to excitation at 440 nm (Table 1). This suggests that some β-carotenes (the only pigments excited in the core complex at 475 nm)

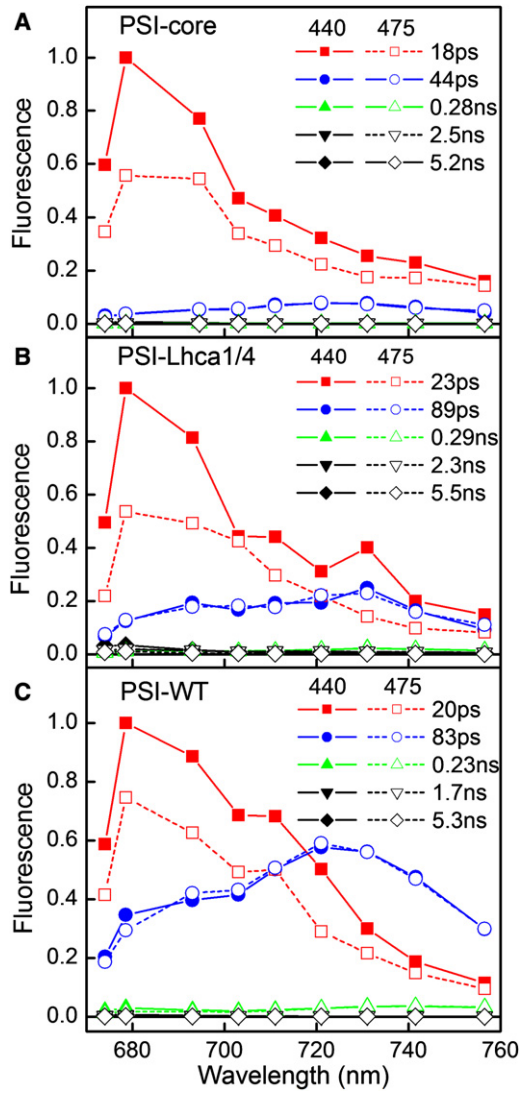

FIGURE 3 TCSPC DAS of PSI core (*A*), PSI-Lhca1/4 (*B*), and PSI-WT (*C*), excitation was at 440 (*solid*) and 475 nm (*dashed*). DAS are normalized to each other based on the area under the red-shifted DAS.

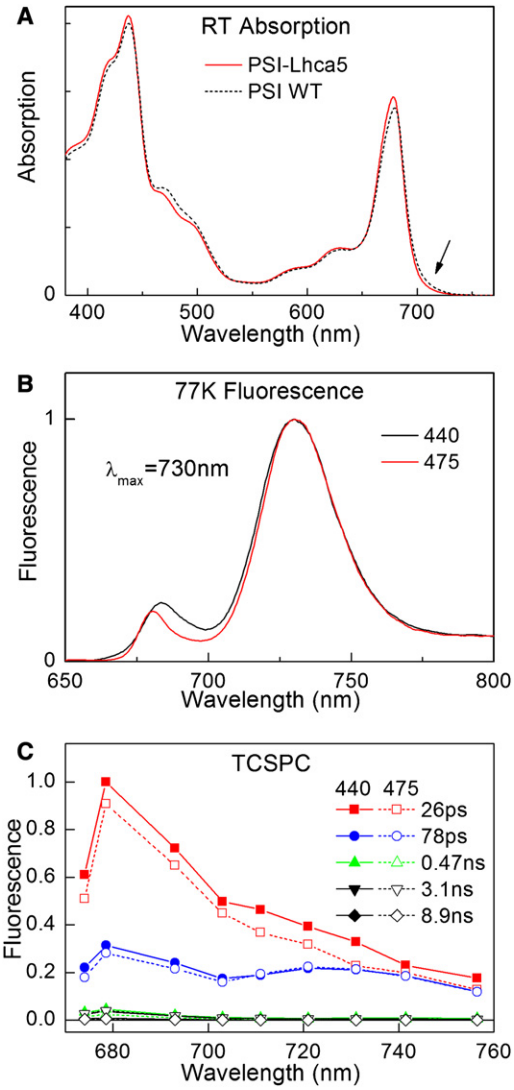

FIGURE 4 RT absorption (*A*), 77 K emission (*B*), and TCSPC DAS (*C*) of PSI-Lhca5. For comparison the absorption spectrum of PSI-WT is also shown (*A*). Spectra are normalized to the number of Chls in the Q_y region (*A*), or the red maximum (*B* and *C*).

are located close to the red forms to which they transfer energy. Because the red Chls have a higher probability to be excited and thus, to generate potentially harmful triplets, a carotenoid in van der Waals contact would be effective in protecting the complex by quenching Chl triplets. By analogy, in LHCI the red forms (Chls603 and 609) are protected by a carotenoid located in the nearby 621 site (28,49).

Analysis of PSI-Lhca1/4 and PSI-WT data reveals two main components: a ~20 ps one with a core-like spectrum, and an 80–90-ps component with an Lhca-like spectrum (720–730 nm). A small additional component associated with a longer lifetime (0.23–0.29 ns) and a red-shifted maximum at ~740 nm is also present. Similar observations were reported for PSI-WT (34,37). The average lifetimes after 475-nm excitation are 55.5 ps for PSI-Lhca1/4 and 58.4 ps for PSI-WT (Table 1), somewhat longer than the 48 ps found with the streak. If the 0.23–0.29-ns lifetime, which was not resolved in the streak experiment, is not taken into account, more similar values of 48 and 53 ps are obtained for PSI-Lhca1/4 and PSI-WT, respectively. Upon more selective excitation of the core (440 nm) the contribution of the ~20 ps decay component increases (Fig. 3 *B* and *C*, Table 1). This results in a decrease of the average lifetime to 46.6 ps for PSI-Lhca1/4 and 52.9 ps for PSI-WT (Table 1). Using the average lifetimes obtained after 440- and 475-nm excitation and the relative fraction of core excitation (Table 1 and Section SI. 2 in the Supporting Material), the lifetimes upon excitation of the core complex ($\overline{\tau}_C$) or LHCI only ($\overline{\tau}_L$) can be calculated (see Materials and Methods and (37), Table 1). For PSI-Lhca1/4 $\overline{\tau}_C$ is shorter than for PSI-WT, in agreement with the lower content of (red) Chls. However, upon

hypothetical excitation of the antenna system the average lifetime ($\overline{\tau}_L$) of PSI-Lhca1/4 becomes somewhat longer than for PSI-WT, indicating that the average EET from LHCI to core ($\overline{\tau}_{L-C}$) takes longer for PSI-Lhca1/4 (31 ps) than for PSI-WT (20 ps). Further analysis (Section SI. 3 in the Supporting Material) shows that EET from Lhca1/4 to the core is slower in PSI-Lhca1/4 than in intact PSI complexes.

The 20 ps $\overline{\tau}_{L-C}$ for PSI-WT are longer than the 9.4 $\pm$ 4.9 ps reported previously for dissolved PSI crystals (37). This difference can be explained by three factors. 1), The lower contribution of red emission for the PSI crystals (37) as compared to PSI-WT described here (Fig. 3), 2), the different values used for the carotenoid to Chl transfer efficiency (see Section SI. 2B in the Supporting Material), and, 3), the different method used to calculate the average lifetimes; in (37) this was based on the average of the lifetimes obtained independently for each detection wavelength, whereas in this study the average lifetimes were based on the relative area under the DAS. The latter method takes into account that some wavelengths contribute stronger to the fluorescence decay than others.

The PSI-Lhca1/5-Lhca2/3 supercomplex

To investigate the effect of the presence/absence of red forms in the intact system, we analyzed a PSI complex in which Lhca4 is substituted by Lhca5. The PSI-Lhca1/5-Lhca2/3 complex has the same supramolecular organization as PSI-WT (43), but a reduced amount of red forms, because Lhca5 does not coordinate them (50).

The absorption spectrum of PSI-Lhca5 is similar to that of PSI-WT (Fig. 4 *A*), but the absorption above 700 nm is less intense. The LT fluorescence emission spectrum of PSI-Lhca5 shows a maximum at 730 nm (Fig. 4 *B*). Because Lhca4 is not present in this sample the 730-nm emission can be entirely attributed to Lhca3, which now contains the lowest energy excited state of the system.

The fluorescence decay was studied with TCSPC after excitation at 440 and 475 nm. The DAS are presented in Fig. 4 *C*: The core-like DAS is associated with a lifetime of 26 ps, somewhat longer than the 20 ps found for PSI-WT. The 78-ps spectrum shows red-shifted emission like the 83-ps component in PSI-WT, but with smaller amplitude (Table 1). This indicates that most of the excitation energy from the Lhca1/5 dimer is rapidly transferred to the core, and thus hardly contributes to the 78-ps spectrum. This results in an average lifetime of only 42.7 ps for PSI-Lhca5, as compared to 58.4 ps in PSI-WT. Upon excitation at 440 nm the average lifetime decreases only with 1.3 ps, giving a $\overline{\tau}_{L-C}$ of 6 ps.

DISCUSSION

In this study we have investigated the effect of individual Lhcas on the EET dynamics of higher plant PSI by analyzing a series of complexes with different antenna size/composition/absorption.

Lhca1/4 and Lhca2/3 have similar effect on PSI decay kinetics

The effect of individual Lhcas on the PSI decay kinetics is discussed in a contradictory way in the literature. On the basis of a comparison of the decay kinetics of intact PSI-LHCI and of PSI largely missing Lhca1/4, it was suggested that EET from Lhca1/4 and Lhca2/3 to the core occurs in a parallel way with similar spectra and kinetics (36). Conversely, in a study on PSI lacking 20–30% of Lhca2/3 it was suggested that this dimer mainly contributes to a red 50-ps DAS, whereas the Lhca1/4 dimer contributes to a stronger red-shifted 120-ps DAS (39). Similarly, based on target analysis of PSI-LHCI fluorescence decay kinetics two red Chl compartments with RT emission maxima at ~720 and ~740 nm (decay lifetimes of 33 and 95 ps) were assigned to Lhca3 and Lhca4, respectively (34). In both studies the amplitude of the "Lhca4"-related DAS was far lower than that of the "Lhca3"-related DAS, which was explained by Slavov et al. (34) by low emitting dipole strength for Lhca4 as is apparent from the small area of the Lhca4 species associated spectrum.

Our collection of PSI particles with different antenna composition is well suited to investigate the effect of the individual Lhcas on the PSI decay kinetics. If the spectra and kinetics of Lhca3 and Lhca4 would indeed differ strongly as proposed (34), then in PSI-Lhca5, where only Lhca3 contributes to the red emission, the lifetime and emission maximum of the red DAS should be considerably shorter than in PSI-Lhca1/4. However, this is not the case: all investigated PSI-Lhca complexes show two main decay components of 20–26 ps (blue spectrum) and 78–89 ps (red spectrum, see Section SI. 4 in the Supporting Material). The relative amplitude of the red DAS correlates with the presence of the red antennae: PSI-WT > PSI-Lhca1/4 > PSI-Lhca5. This relation qualitatively shows that Lhca3 and Lhca4 contribute about equally to the ~80-ps DAS, consistent with the similar absorption and emission properties of Lhca3 and Lhca4 (5,26). The data disprove the assignments in (34,39) in which spectra with very different amplitude, emission maxima, and lifetimes were assigned to Lhca3 and Lhca4.

Nevertheless, as observed previously (34,35,37,39), a small second red DAS was resolved for PSI-WT and PSI-Lhca1/4 (Section SI. 4 in the Supporting Material, Fig. 3, Table 1). As our data show that this heterogeneity of the fluorescence decay cannot be explained by a very different coupling of Lhca3 and Lhca4 to the core, we propose that it might be attributed to the large inhomogeneous broadening of the red forms (16,18,51).

Fast energy transfer from the blue antenna to the core

To study in more detail the effect of the red forms, we have used PSI-Lhca5, with the same antenna size and organization as WT, but with reduced red forms content. EET from the antenna to the core occurs substantially faster than in PSI-WT. Because the only difference is the replacement of red-Lhca4 by blue-Lhca5, it can be concluded that the blue antennae, namely Lhca1, Lhca2, and Lhca5, are responsible for fast EET to the core. Thus, the main barrier for EET between LHCI and core are the low-energy Chls, as was suggested based on a temperature dependence (13) and modeling (34) of PSI excitation energy trapping kinetics. At variance with a previous suggestion (36) the data show that EET from Lhca5 to the core is very efficient.

Impact of the red forms on the effective trapping rate

To investigate the effect of LHCI on the average fluorescence lifetime, we compare $<\tau>$ = ~22 ps of PSI-core to $\overline{\tau}_L$ = ~65 ps of PSI-WT upon selective LHCI excitation. This shows that LHCI slows down the effective trapping rate by a factor of three, in agreement with previous results (33,34). Because PSI-WT coordinates ~1.5 times more Chls *a* than the core (40,50), for well coupled isoenergetic Chls *a* it can be assumed that $\overline{\tau}_L$ increases with the same factor (from 22 to 33 ps). The additional 2× increase to 65 ps can be ascribed to the slow energetically uphill EET from the red forms to the trap. Treating the data of Engelman et al. (33) in the same way also gives a 2× increase of the trapping time due to the red forms, and a similar increase of 2.3× was reported by Slavov et al (34) based on their kinetic modeling results.

Comparing the effect of the red forms on $\overline{\tau}_L$ of PSI-Lhca5, which only contains the red forms of Lhca3 (17,43), and PSI-WT, allows to disentangle the effect of Lhca3 and Lhca4. The effective trapping time of PSI-Lhca5 is increased by a factor of 1.4 (from 33 to 45 ps) compared to the case of isoenergetic pigments. This suggests that ~40% of the increase in trapping time in PSI-WT can be ascribed to the red form of Lhca3, and 60% to that of Lhca4.

If a dissipative rate of 0.4/ns (as found for LHCI (26)) is assumed for PSI in the absence of charge separation, it follows that the trapping efficiencies of core, PSI-WT, and PSI-Lhca5 are 99.1%, 97.4%, and 98.2%, respectively. Thus, even though Lhca3 and Lhca4 severely slow down the trapping rate, the effect on trapping efficiency is limited. It can be speculated that Nature has searched for an optimal PSI light harvesting, using as much of the solar spectrum as possible while remaining to work at an extremely high efficiency. It should be noted that, although the red forms are only responsible for a small fraction (4–5%) of light absorption under a normal daylight environment, they may be responsible for up to 40% of the light absorption under deep shade-light conditions (30). Thus, especially under shade conditions the small drop in PSI efficiency is negligible compared to the advantage of the increased absorption.

All Lhcas contribute equally to EET to the core

The association of LHCI to the core gives rise to a long trapping lifetime (Figs. 2 and 3), which is reflecting slow EET between (part of) LHCI and the core. This has been explained by i), difficulties in EET between the complexes and/or ii), by the red forms of LHCI (13,33–36,39,40). If intermonomer EET within Lhca1/4 and Lhca2/3 takes place on a faster timescale than transfer to the core, which can occur if (i) is dominating, than the EET occurs from an equilibrated system and can be described by a single rate constant for each dimer, as assumed in (36,37,39). However, if (ii) has the most important contribution, then EET from LHCI to the core is slower for the complexes with more red-shifted emission (34), thus $k_{Lhca4} < k_{Lhca3} << k_{Lhca2} < k_{Lhca1}$ (10,17). The experimental evidence for fast EET from the blue Lhcas to the core (discussed above) indicates that (i) does not play a significant role and that (ii) mainly contributes to the slow trapping in PSI-LHCI.

This means that the rates of transfer from the individual Lhcas to the core can be estimated based on energetic considerations. If it is assumed that 1), energy equilibration within Lhca is faster than EET between Lhca and core, and 2), EET from the core to all Lhcas occurs with the same rate, then the ratio of the EET rates from individual Lhca's to the core (formula 2) can be derived from the detailed balance equation (see Section SI. 5A in the Supporting Material). The validity of assumption (1) will be discussed below. The second assumption is justified because the Förster overlap integral between the emission of a bulk Chl and the absorption of a red-shifted Chl (with an oscillator strength of 2 Chls (26), see Section SI. 5B in the Supporting Material) is similar to the overlap with a bulk Chl; furthermore, in absorption the red forms do not play such an important role (as compared to fluorescence).

$$\frac{k_{a4C}}{k_{a1C}} = \frac{k_{a4a1}}{k_{a1a4}} \quad \text{and} \quad \frac{k_{a3C}}{k_{a2C}} = \frac{k_{a3a2}}{k_{a2a3}}, \tag{2}$$

where $k_{a\#C}$ is the rate of transfer from Lhca# to the core, and $k_{a\#a^*}$ is the rate of transfer from Lhca# to Lhca*, and $k_{a^*a\#}$ is the backward rate.

The intermonomer EET rates of Lhca1/4 and Lhca2/3 in solution have been resolved in (26). Similar ratios of transfer rates are expected when the dimers are coordinated to the core complex; it thus follows that k_{a1C} is four times k_{a4C} and k_{a2C} is three times k_{a3C} (26). For PSI-WT we obtained an antenna-core migration rate of 50/ns from the analysis of the TCSPC experiments. Assuming equal average rates for both dimers and equal initial excitation of the Lhcas (which is reasonable based on the similar absorption properties of

the dimers (5)) we obtain k_{a1C} and k_{a2C} 80 and 75/ns, and k_{a3C} and k_{a4C} 25 and 20/ns, respectively (see Fig. 6). The faster transfer from Lhca3 compared to Lhca4 might explain the slightly shorter lifetime (78 ps) of the red DAS found for PSI-Lhca5, and slightly longer lifetime for PSI-Lhca1/4 (89 ps), compared to PSI-WT (83 ps). The fastest transfer occurs with a rate of 80/ns, a factor of ~2.5 slower than the slowest equilibration process in Lhca4 and Lhcbs (52,53), indicating that assumption 1) is reasonable. However, it cannot be excluded that a fraction of the excitation energy is transferred to the core before energy equilibration within the Lhcas is completed. In this case the effective average transfer time from the high-energy forms would be somewhat faster and that of the red forms somewhat slower than found with our current model. This might explain the faster transfer obtained for PSI-Lhca5 as compared to the transfer from blue Lhca in PSI-WT.

The EET from the blue Lhca to the core and to the red Lhca in the dimer is fast, while both transfer rates are slow for the red Lhcas (see above and (26)). Therefore, upon equal excitation, both blue and red Lhcas transfer the same fraction of their absorbed energy (>60%) directly to the core, while the rest (<40%) is transferred to the other Lhca in the dimer (see Fig. 6).

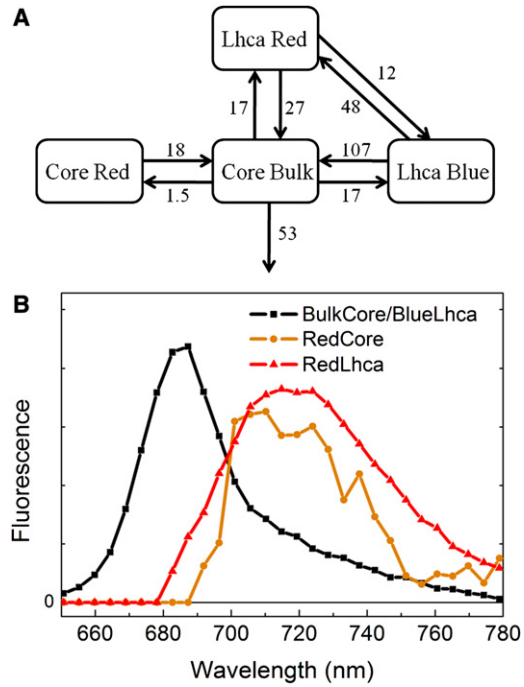

FIGURE 5 Target analysis of PSI-LHCI kinetics. (*A*) Compartmental model of PSI-LHCI, with EET rates in /ns. (*B*) Species associated spectra of the compartments.

Target analysis: PSI model

To obtain a complete picture of the transfer and trapping kinetics of PSI-LHCI, target analysis was performed on the streak camera data. The data were fitted to a compartmental model where the compartments represent a simplified picture of the different parts of the system. This provides the spectra of, and the transfer rates between the different compartments (see (48) for details).

First, the decay of the PSI core was modeled. Its detailed trapping kinetics is discussed controversially in the literature (see for example (54) vs. (55)), and is beyond the scope of this work. We describe the kinetics with a simple two compartment model: one for bulk Chls from which trapping occurs and one for red Chls (Fig. 5 *A*). An apparent trapping rate of 53/ns was obtained, in good agreement with 56/ns, which was proposed as a general trapping rate for bulk Chls in PSI core particles (32). In the second step PSI-WT is modeled, assuming that the core kinetics remain the same. Because the emission spectra at RT of Lhca1 and Lhca2 and of Lhca3 and Lhca4 (10,17,26) are similar, we introduce only one blue (Lhca1,2) and one red (Lhca3,4) compartment in the model. The ratio of EET from the blue antenna to the core is forced to be four times faster than that of the red antenna, similar to the ratios used for the analysis of the TCSPC data. The transfer rates between blue and red antenna were obtained from the analysis of the Lhca1/4 dimer (26). Although the modeling is coarse-grained, it provides a satisfactory description of the data (Fig. 5, Section SI. 6 in the Supporting Material). The emission maximum of the red Lhcas is found at 720 nm, in good agreement with our previous work on isolated LHCI dimers (see Lhca3 and Lhca4 spectra (26)). The evolution of the excitation concentrations on the different compartments are shown in Section SI. 7 in the Supporting Material. The rates of transfer from antenna to core (blue 107/ns, red 27/ns) are similar but somewhat faster than the ones based on the analysis of TCSPC data (blue 75 80/ns, red 20–25/ns).

Target analysis was also performed for PSI-Lhca1/4 (Section SI. 8 in the Supporting Material). The rate of transfer from antenna to core was estimated to be 75% of that in PSI-WT, in agreement with the larger $\overline{\tau}_{L-C}$ obtained from the TCSPC data. The ratio between forward and backward transfer between core and Lhcas is half in PSI-Lhca1/4 as compared to PSI-WT, which is expected when the Lhca antenna size is reduced by a factor of two.

Two previous studies have addressed the rates of transfer from Lhca3 and Lhca4 to the core. In Ihalainen et al. (40) a 7/ns red Lhca to core rate was reported, thus ~4 times slower than the 27/ns obtained from our analysis. However, an unusually large LHCI loss channel of 7/ns was also needed to describe the data, while the isolated dimers decay with a lifetime of 0.4/ns (26,56), thus suggesting that the model does not give a realistic description of the kinetics. In the study of Slavov et al. (34) the reported values of 14 and 36/ns for red Lhca to core are comparable to the 27/ns obtained here but the decay of Lhca3 and Lhca4 was described with very different spectra and kinetics, while our data indicate that this cannot be the case.

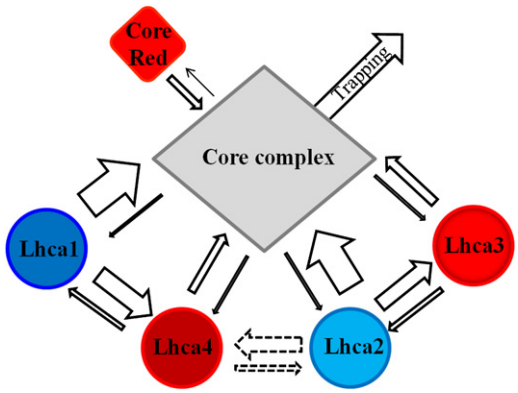

FIGURE 6 Schematic presentations of energy transfer and trapping in PSI-LHCI. Thickness of the arrows indicates the rates. The transfer rate between Lhca2 and Lhca4 could not be estimated from our target analysis, but, based on structural data, it has been suggested to be similar to the intradimer transfer rates (1,58).

SUMMARIZING CONCLUSION

Combining streak camera and TCSPC measurements we investigated excitation energy transfer and trapping kinetics of higher plant PSI-LHCI, taking into account the transfer rates from, to, and between individual Lhcas. Fig. 6 summarizes the results:

- Transfer from Lhca1 and Lhca2 to the core occurs very fast (~100/ns) and faster than energy equilibration between the Lhcas.
- Excitation energy can only "slowly" (~25/ns) escape from Lhca3 and Lhca4 to the core.
- Each Lhca contributes about equally to the transfer to the core.
- The spectra of Lhca3 and Lhca4 are similar, with a red-emission maximum at 715–720 nm.
- The red forms of Lhca3 and Lhca4 slow down the effective PSI trapping rate in a comparable manner, and together by ~2 times.

SUPPORTING MATERIAL

Eight sections, with 10 figures, plus references are available at http://www.biophysj.org/biophysj/supplemental/S0006-3495(11)00775-2.

The authors thank Arie van Hoek and Rob Koehorst for excellent technical support and Stefan Jansson for providing the Lhca mutant lines.

This work was supported by De Nederlandse Organisatie voor Wetenschappelijk Onderzoek, Earth and Life Sciences, through a Vidi grant (to R.C.).

REFERENCES

1. Ben-Shem, A., F. Frolow, and N. Nelson. 2003. Crystal structure of plant photosystem I. *Nature.* 426:630–635.
2. Jordan, P., P. Fromme, …, N. Krauss. 2001. Three-dimensional structure of cyanobacterial photosystem I at 2.5 A resolution. *Nature.* 411:909–917.
3. Boekema, E. J., P. E. Jensen, …, J. P. Dekker. 2001. Green plant photosystem I binds light-harvesting complex I on one side of the complex. *Biochemistry.* 40:1029–1036.
4. Croce, R., T. Morosinotto, …, R. Bassi. 2002. The Lhca antenna complexes of higher plants photosystem I. *Biochim. Biophys. Acta.* 1556:29–40.
5. Wientjes, E., and R. Croce. 2011. The light-harvesting complexes of higher-plant Photosystem I: Lhca1/4 and Lhca2/3 form two red-emitting heterodimers. *Biochem. J.* 433:477–485.
6. Ganeteg, U., F. Klimmek, and S. Jansson. 2004. Lhca5—an LHC-type protein associated with photosystem I. *Plant Mol. Biol.* 54:641–651.
7. Jansson, S. 1999. A guide to the Lhc genes and their relatives in *Arabidopsis*. *Trends Plant Sci.* 4:236–240.
8. Amunts, A., H. Toporik, …, N. Nelson. 2010. Structure determination and improved model of plant photosystem I. *J. Biol. Chem.* 285:3478–3486.
9. Croce, R., and R. Bassi. 1998. The light-harvesting complex of Photosystem I: pigment composition and stoichiometry. *In* Photosynthesis: Mechanisms and Effects, *Vol. 1*. G. Garab, editor. Kluwer Academic Publishers, Dordrecht, The Netherlands. 421–424.
10. Schmid, V. H. R., K. V. Cammarata, …, G. W. Schmidt. 1997. In vitro reconstitution of the photosystem I light-harvesting complex LHCI-730: heterodimerization is required for antenna pigment organization. *Proc. Natl. Acad. Sci. USA.* 94:7667–7672.
11. Gobets, B., and R. van Grondelle. 2001. Energy transfer and trapping in photosystem I. *Biochim. Biophys. Acta. Bioenerg.* 1507:80–99.
12. Melkozernov, A. N. 2001. Excitation energy transfer in Photosystem I from oxygenic organisms. *Photosynth. Res.* 70:129–153.
13. Jennings, R. C., G. Zucchelli, …, F. M. Garlaschi. 2003. The photochemical trapping rate from red spectral states in PSI-LHCI is determined by thermal activation of energy transfer to bulk chlorophylls. *Biochim. Biophys. Acta. Bioenerg.* 1557:91–98.
14. Nelson, N., and C. F. Yocum. 2006. Structure and function of photosystems I and II. *Annu. Rev. Plant Biol.* 57:521–565.
15. Croce, R., G. Zucchelli, …, R. C. Jennings. 1998. A thermal broadening study of the antenna chlorophylls in PSI-200, LHCI, and PSI core. *Biochemistry.* 37:17355–17360.
16. Ihalainen, J. A., M. Ratsep, P. E. Jensen…, 2003. Red spectral forms of chlorophylls in green plant PSI - a site-selective and high-pressure spectroscopy study. *J. Phys. Chem. B.* 107:9086–9093.
17. Castelletti, S., T. Morosinotto, …, R. Croce. 2003. Recombinant Lhca2 and Lhca3 subunits of the photosystem I antenna system. *Biochemistry.* 42:4226–4234.
18. Croce, R., A. Chojnicka, …, R. van Grondelle. 2007. The low-energy forms of photosystem I light-harvesting complexes: spectroscopic properties and pigment-pigment interaction characteristics. *Biophys. J.* 93:2418–2428.
19. Croce, R., T. Morosinotto, …, R. Bassi. 2004. Origin of the 701-nm fluorescence emission of the Lhca2 subunit of higher plant photosystem I. *J. Biol. Chem.* 279:48543–48549.
20. Morosinotto, T., S. Castelletti, …, R. Croce. 2002. Mutation analysis of Lhca1 antenna complex. Low energy absorption forms originate from pigment-pigment interactions. *J. Biol. Chem.* 277:36253–36261.
21. Liu, Z., H. Yan, …, W. Chang. 2004. Crystal structure of spinach major light-harvesting complex at 2.72 A resolution. *Nature.* 428:287–292.
22. Mozzo, M., T. Morosinotto, …, R. Croce. 2006. Probing the structure of Lhca3 by mutation analysis. *Biochim. Biophys. Acta. Bioenerg.* 1757:1607–1613.
23. Morosinotto, T., M. Mozzo, …, R. Croce. 2005. Pigment-pigment interactions in Lhca4 antenna complex of higher plants photosystem I. *J. Biol. Chem.* 280:20612–20619.
24. Morosinotto, T., J. Breton, …, R. Croce. 2003. The nature of a chlorophyll ligand in Lhca proteins determines the far red fluorescence emission typical of photosystem I. *J. Biol. Chem.* 278:49223–49229.

25. Romero, E., M. Mozzo, …, R. Croce. 2009. The origin of the low-energy form of photosystem I light-harvesting complex Lhca4: mixing of the lowest exciton with a charge-transfer state. *Biophys. J.* 96:L35–L37.

26. Wientjes, E., I. H. M. van Stokkum, …, R. Croce. 2011. Excitation-energy transfer dynamics of higher plant photosystem I light-harvesting complexes. *Biophys. J.* 100:1372–1380.

27. Croce, R., G. Zucchelli, …, R. C. Jennings. 1996. Excited state equilibration in the photosystem I-light-harvesting I complex: P700 is almost isoenergetic with its antenna. *Biochemistry.* 35:8572–8579.

28. Carbonera, D., G. Agostini, …, R. Bassi. 2005. Quenching of chlorophyll triplet states by carotenoids in reconstituted Lhca4 subunit of peripheral light-harvesting complex of photosystem I. *Biochemistry.* 44:8337–8346.

29. Trissl, H. W. 1993. Long-wavelength absorbing antenna pigments and heterogeneous absorption-bands concentrate excitons and increase absorption cross-section. *Photosynth. Res.* 35:247–263.

30. Rivadossi, A., G. Zucchelli, …, R. C. Jennings. 1999. The importance of PSI chlorophyll red forms in light-harvesting by leaves. *Photosynth. Res.* 60:209–215.

31. Karapetyan, N. V., A. R. Holzwarth, and M. Rögner. 1999. The photosystem I trimer of cyanobacteria: molecular organization, excitation dynamics and physiological significance. *FEBS Lett.* 460:395–400.

32. Gobets, B., I. H. M. van Stokkum, …, R. van Grondelle. 2001. Time-resolved fluorescence emission measurements of photosystem I particles of various cyanobacteria: a unified compartmental model. *Biophys. J.* 81:407–424.

33. Engelmann, E., G. Zucchelli, …, R. C. Jennings. 2006. Influence of the photosystem I-light harvesting complex I antenna domains on fluorescence decay. *Biochemistry.* 45:6947–6955.

34. Slavov, C., M. Ballottari, …, A. R. Holzwarth. 2008. Trap-limited charge separation kinetics in higher plant photosystem I complexes. *Biophys. J.* 94:3601–3612.

35. Croce, R., D. Dorra, …, R. C. Jennings. 2000. Fluorescence decay and spectral evolution in intact photosystem I of higher plants. *Biochemistry.* 39:6341–6348.

36. Ihalainen, J. A., F. Klimmek, …, J. P. Dekker. 2005. Excitation energy trapping in photosystem I complexes depleted in Lhca1 and Lhca4. *FEBS Lett.* 579:4787–4791.

37. van Oort, B., A. Amunts, …, R. Croce. 2008. Picosecond fluorescence of intact and dissolved PSI-LHCI crystals. *Biophys. J.* 95:5851–5861.

38. Ihalainen, J. A., R. Croce, …, R. van Grondelle. 2005. Excitation decay pathways of Lhca proteins: a time-resolved fluorescence study. *J. Phys. Chem. B.* 109:21150–21158.

39. Ihalainen, J. A., P. E. Jensen, …, J. P. Dekker. 2002. Pigment organization and energy transfer dynamics in isolated photosystem I (PSI) complexes from *Arabidopsis thaliana* depleted of the PSI-G, PSI-K, PSI-L, or PSI-N subunit. *Biophys. J.* 83:2190–2201.

40. Ihalainen, J. A., I. H. M. van Stokkum, …, J. P. Dekker. 2005. Kinetics of excitation trapping in intact Photosystem I of *Chlamydomonas reinhardtii* and *Arabidopsis thaliana*. *Biochim. Biophys. Acta.* 1706: 267–275.

41. Klimmek, F., U. Ganeteg, …, S. Jansson. 2005. Structure of the higher plant light harvesting complex I: in vivo characterization and structural interdependence of the Lhca proteins. *Biochemistry.* 44:3065–3073.

42. Morosinotto, T., M. Ballottari, …, R. Bassi. 2005. The association of the antenna system to photosystem I in higher plants. Cooperative interactions stabilize the supramolecular complex and enhance red-shifted spectral forms. *J. Biol. Chem.* 280:31050–31058.

43. Wientjes, E., G. T. Oostergetel, …, R. Croce. 2009. The role of Lhca complexes in the supramolecular organization of higher plant photosystem I. *J. Biol. Chem.* 284:7803–7810.

44. Ganeteg, U., C. Külheim, …, S. Jansson. 2004. Is each light-harvesting complex protein important for plant fitness? *Plant Physiol.* 134: 502–509.

45. Ganeteg, U., …, S. Strand A, Jansson. 2001. The properties of the chlorophyll *a*/*b*-binding proteins Lhca2 and Lhca3 studied in vivo using antisense inhibition. *Plant Physiol.* 127:150–158.

46. Somsen, O. J., L. B. Keukens, …, H. van Amerongen. 2005. Structural heterogeneity in DNA: temperature dependence of 2-aminopurine fluorescence in dinucleotides. *ChemPhysChem.* 6:1622–1627.

47. van Oort, B., S. Murali, E. Wientjes…, 2009. Ultrafast resonance energy transfer from a site-specifically attached fluorescent chromophore reveals the folding of the N-terminal domain of CP29. *Chem. Phys.* 357:113–119.

48. Stokkum, I. H. M., D. S. Larsen, and R. Grondelle. 2004. Global and target analysis of time-resolved spectra. *Biochim. Biophys. Acta. Bioenerg.* 1657:82–104.

49. Croce, R., M. Mozzo, …, R. Bassi. 2007. Singlet and triplet state transitions of carotenoids in the antenna complexes of higher-plant photosystem I. *Biochemistry.* 46:3846–3855.

50. Storf, S., S. Jansson, and V. H. R. Schmid. 2005. Pigment binding, fluorescence properties, and oligomerization behavior of Lhca5, a novel light-harvesting protein. *J. Biol. Chem.* 280:5163–5168.

51. Gobets, B., H. van Amerongen, R. Monshouwer…, 1994. Polarized site-selected fluorescence spectroscopy of isolated photosystem-I particles. *Biochim. Biophys. Acta. Bioenerg.* 1188:75–85.

52. Gibasiewicz, K., R. Croce, …, R. van Grondelle. 2005. Excitation energy transfer pathways in Lhca4. *Biophys. J.* 88:1959–1969.

53. Croce, R., M. G. Müller, …, A. R. Holzwarth. 2003. Chlorophyll *b* to chlorophyll *a* energy transfer kinetics in the CP29 antenna complex: a comparative femtosecond absorption study between native and reconstituted proteins. *Biophys. J.* 84:2508–2516.

54. Holzwarth, A. R., M. G. Müller, …, W. Lubitz. 2006. Ultrafast transient absorption studies on photosystem I reaction centers from Chlamydomonas reinhardtii. 2: mutations near the P700 reaction center chlorophylls provide new insight into the nature of the primary electron donor. *Biophys. J.* 90:552–565.

55. Shelaev, I. V., F. E. Gostev, M. D. Mamedov…, 2010. Femtosecond primary charge separation in *Synechocystis* sp. PCC 6803 photosystem I. *Biochim. Biophys. Acta. Bioenerg.* 1797:1410–1420.

56. Gobets, B., J. T. M. Kennis, J. A. Ihalainen…, 2001. Excitation energy transfer in dimeric light harvesting complex I: a combined streak-camera/fluorescence upconversion study. *J. Phys. Chem. B.* 105:10132–10139.

57. Amunts, A., O. Drory, and N. Nelson. 2007. The structure of a plant photosystem I supercomplex at 3.4 A resolution. *Nature.* 447:58–63.

58. Sener, M. K., C. Jolley, …, K. Schulten. 2005. Comparison of the light-harvesting networks of plant and cyanobacterial photosystem I. *Biophys. J.* 89:1630–1642.